Acta Crystallographica Section D
Biological Crystallography
ISSN 0907-4449

An icosahedral assembly of the light-harvesting chlorophyll *a*/*b* protein complex from pea chloroplast thylakoid membranes

Tomoya Hino,[a] Eiji Kanamori,[a] Jian-Ren Shen[b] and Tsutomu Kouyama[a]*

[a]Department of Physics, Graduate School of Science, Nagoya University, Nagoya 464-8602, Japan, and [b]RIKEN Harima Institute/SPring-8, Kouto, Mikazuki, Hyogo 679-5198, Japan

Correspondence e-mail: kouyama@bio.phys.nagoya-u.ac.jp

Received 4 January 2003
Accepted 9 February 2004

PDB Reference: light-harvesting chlorophyll *a*/*b* protein complex, 1vcr, r1vcrsf.

When the light-harvesting chlorophyll *a*/*b* protein complex (LHC-II) from pea thylakoid membranes is co-crystallized with native lipids, an octahedral crystal that exhibits no birefringence is obtained. Cryogenic electron micrographs of a crystal edge showed the crystal to be made up of hollow spherical assemblies with a diameter of 250 Å. X-ray diffraction data at 9.5 Å resolution revealed the spherical shell of LHC-II to have icosahedral symmetry. A $T = 1$ icosahedral model of LHC-II, in which the stromal surface of the protein faces outward, was constructed using the previously reported structure of the LHC-II trimer [Kühlbrandt *et al.* (1994), *Nature (London)*, **367**, 614–621]. The present result shows the first example of a well ordered three-dimensional crystal of icosahedral proteoliposomes.

1. Introduction

An increasing number of proteins have been shown to self-assemble into a regular hollow polyhedral form. In most spherical virus capsids, a multiple of 60 subunits are arranged with icosahedral symmetry (Casper & Klug, 1963; Crowther *et al.*, 1970; Heinz & Allison, 2001). Clathrin is a non-virus protein that assembles into a polyhedral cage on the cytoplasmic side of a membrane (Smith *et al.*, 1998; Pearse *et al.*, 2000). $T = 1$ icosahedral geometry has recently been found in several multienzyme complexes, *e.g.* pyruvate dehydrogenase complexes (Izard *et al.*, 1999; Domingo *et al.*, 2001), riboflavin synthase/lumazine synthase complexes (Persson *et al.*, 1999; Zhang *et al.*, 2001) and tricorn protease (Walz *et al.*, 1999; Brandstetter *et al.*, 2001). Recent studies have shown that some membrane proteins organize into spherical shells. The transmembrane protein bacteriorhodopsin, which functions as a light-driven proton pump, is the first such example. When its two-dimensional crystal (called purple membrane) is incubated with a small amount of detergent, the membrane converts to uniformly sized spherical vesicles with the trimeric bacteriorhodopsin–lipid complexes arranged in an icosahedral lattice (Kouyama *et al.*, 1994). The second example is the E1–E2 complex of alphavirus, which forms an icosahedral shell without help of the scaffolding capsid protein (Forsell *et al.*, 2000). The assembly process may be different for these two examples, but the principal architecture is similar: the trimeric complexes are the basic blocks of the icosahedral structures. It is interesting to ask whether other membrane proteins that form stable trimeric complexes can assemble into a regular hollow structure when they are forced to concentrate in restricted regions of biological membranes.

Light-harvesting chlorophyll *a*/*b* protein complexes (LHC-II), the most abundant membrane-spanning proteins in the thylakoid membranes of green algae and higher plants,

gather solar energy. The major component of LHC-II in higher plants mostly consists of a 25 kDa polypeptide chain, which binds nearly equal numbers of chlorophyll *a* and *b* (Kühlbrandt *et al.*, 1994). This protein has been shown to form a stable trimeric structure under physiological conditions (Kühlbrandt, 1994). Previously, Kühlbrandt reported two crystal forms of LHC-II from thylakoid membranes of pea chloroplasts (Kühlbrandt, 1987): a hexagonal crystal and an octahedral crystal. Although these crystals were not used for structural determination of LHC-II owing to limited X-ray diffraction resolution, we were interested in these crystals because of their apparent similarities to the bacteriorhodopsin crystals produced in the presence of native lipids (Kouyama *et al.*, 1994; Takeda *et al.*, 1998). The octahedral crystal of LHC-II has a large unit cell (361–387 Å) and exhibits no birefringence; these properties are shared by the octahedral crystal of bacteriorhodopsin (747 Å), which is composed of polyhedral assemblies. The hexagonal crystal of LHC-II appeared to be composed of stacked membranes; this was also observed in the *P*622 crystal of bacteriorhodopsin (Sato *et al.*, 1999; Matsui *et al.*, 2002). Additionally, both these proteins crystallize under similar conditions. The coexistence of native lipids is essential for the crystal growth of these two membrane proteins (Takeda *et al.*, 1998; Nussberger *et al.*, 1993). Furthermore, like bacteriorhodopsin, LHC-II forms a trimeric structure under physiological conditions (Nussberger *et al.*, 1993).

From these similarities, it appears that the underlying crystallization mechanism is similar for these two membrane proteins. In order to investigate this possibility, we improved the crystallization procedure of LHC-II so as to obtain crystals suitable for crystallographic analyses. We have obtained an octahedral crystal that diffracts to 8 Å resolution and a hexagonal crystal that diffracts to beyond 3 Å resolution. The hexagonal crystal seems to be suitable for construction of an atomic model of LHC-II, but further refinement of the crystallization conditions is still required. In this study, we address the structural analysis of the octahedral crystal of LHC-II and discuss the mechanism of formation of the vesicular assembly found in this crystal.

2. Materials and methods

2.1. Purification and crystallization of LHC-II

LHC-II was purified from thylakoid membranes of pea chloroplasts according to Burke *et al.* (1978), with modifications made by Kühlbrandt (1987). Briefly, chloroplast thylakoid membranes were solubilized with 0.5%(*w*/*v*) Triton X-100 at a chlorophyll concentration of 0.5 mg ml^{-1} and LHC-II was separated from other proteins using sucrose linear-density gradient centrifugation. LHC-II was then precipitated by adding solid KCl to a final concentration of 300 m*M*. The chlorophyll concentration was determined according to Arnon (1949).

For preparation of the octahedral crystal of LHC-II, the protocol reported by Kühlbrandt (1987) was modified. After investigating a variety of crystallization conditions, we found that addition of polyethylene glycol (PEG 4000) to be effective in yielding crystals that diffract X-rays to 8 Å. Our final crystallization protocol was as follows: the purified protein at a chlorophyll concentration of 4 mg ml^{-1} was solubilized with 0.8%(*w*/*v*) nonyl glucoside (*n*-nonyl-β,D-glucopyranoside, Fluka) in the presence of 10 m*M* HEPES pH 7.0. 5 µl protein solution was mixed with an equal volume of crystallization buffer containing 0.4%(*w*/*v*) nonyl glucoside, 35 m*M* KCl, 6% PEG 4000, 10% xylitol and 10 m*M* HEPES pH 7.0. After centrifugation at 10 000*g*, the supernatant was slowly concentrated at 283 K by the hanging-drop vapour-diffusion method using a reservoir solution containing 35 m*M* KCl, 6% PEG 4000, 10% xylitol and 10 m*M* HEPES pH 7.0. Within a week, octahedral crystals grew to dimensions of 0.3 × 0.3 × 0.3 mm. For cryogenic diffraction experiments, a single crystal was soaked in a solution consisting of 35 m*M* KCl, 8% PEG 4000, 40% xylitol and 10 m*M* HEPES pH 7.0 for 10 min and rapidly cooled by immersing into liquid propane.

2.2. Electron microscopy

Transmission electron microscopy was performed with a JEM2010 (Jeol) electron microscope operated at 200 kV. A 3 µl suspension containing small octahedral crystals of LHC-II was mounted on a carbon-coated grid that had been rendered hydrophilic by glow discharge. Excess liquid was removed with a filter paper (No. 2, Whatman) and the grid was plunged into liquid propane and transferred to a cryotransfer stage (Oxford CT3500). An edge part of a small crystal was exposed to an electron beam at $\sim$10 e Å^{-2} for 1 s and a micrographic image was recorded using SO-163 films (Kodak). Electron micrographs were digitized with a Minolta DiMAGE Scan Multi PRO Model AF-5000.

2.3. X-ray crystallographic analysis

X-ray diffraction data were collected on a MAR CCD detector at beamline BL41XU of SPring-8. The intensity data were indexed and integrated using *MOSFLM* (Steller *et al.*, 1997) and further processed using *SCALA* and *TRUNCATE* from the *CCP*4 program package (Collaborative Computational Project, Number 4, 1994). The self-rotation function was calculated using the program *GLRF* (Tong & Rossmann, 1990). The twinning fraction of a crystal was estimated by the method of Yeates (1997). To determine the structure of the spherical shell assembly of LHC-II, the polyalanine model of LHC-II (amino-acid residues 55–89, 123–143 and 170–214 and 12 tetrapyrols: seven chlorophyll *a* and five chlorophyll *b*) reported by Kühlbrandt *et al.* (1994) was used. The crystal used was found to be merohedrally twinned, implying that conventional structural analyses cannot be performed. Thus, we chose to begin by evaluating various trial models which were built on the assumption that 20 trimers of LHC-II are arranged in a $T = 1$ icosahedral lattice. The structure amplitudes of the *hkl* and *hlk* reflections, $F_c(hkl)$ and $F_c(hlk)$, were calculated for each trial model and the calculated amplitude $F_c^{twin}(hkl) = \{[|F_c(hkl)|^2 + |F_c(hlk)|^2]/2\}^{1/2}$ was compared with the observed amplitude $F_o^{twin} = \{[I_o(hkl) + I_o(hlk)]/2\}^{1/2}$, where

$I_o(hkl)$ and $I_o(hlk)$ are the observed intensities of the hkl and hlk reflections, respectively. Finally, the crystallographic R value $[\sum_{hkl} \left|k|F_c^{twin}| \exp(-B|\mathbf{s}|^2/4) - |F_o^{twin}|\right| / |F_o^{twin}|]$ was evaluated for all the trial models using the software *CNS* (Brünger *et al.*, 1998) and the final model providing the lowest R_{cryst} value was determined. To refine the structural model under icosahedral symmetry constraints, we performed a rigid-body refinement of the individual LHC-II monomer using the reflection intensities obtained by the detwinning procedure: $I_{detwin}(hkl) = [I_{twin}(hkl) + I_c(hkl) - I_c(hlk)]/2$, where I_{twin} is the observed intensity and I_c is the intensity calculated from the icosahedral model. The icosahedral model thus constructed was checked graphically using *XtalView* (McRee, 1993).

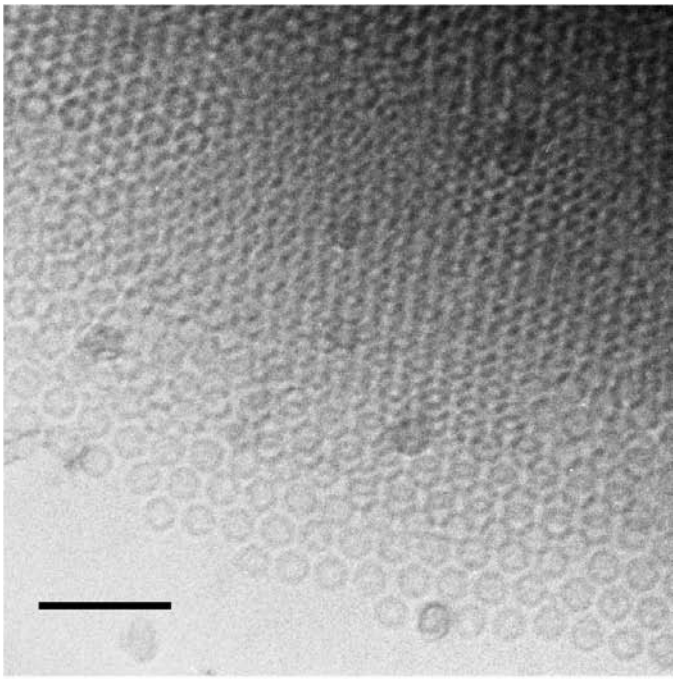

(*a*)

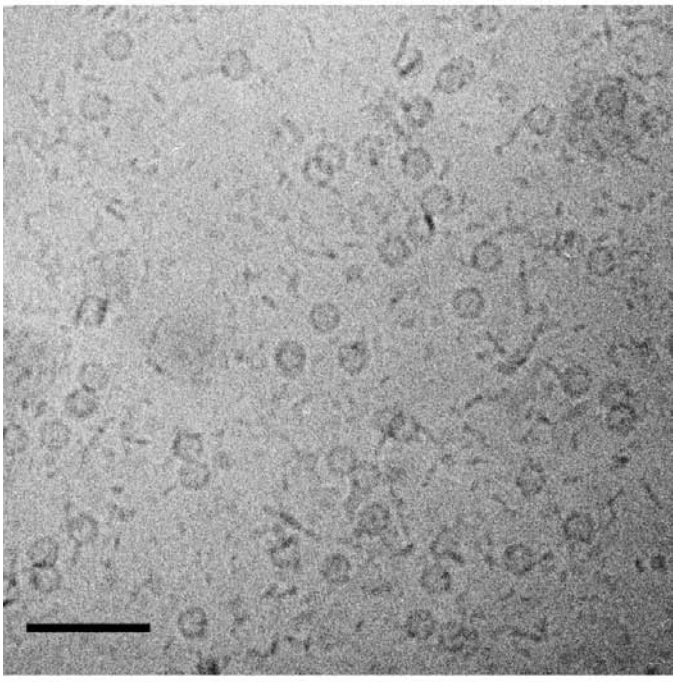

(*b*)

Figure 1
Electron micrographs of the vesicular assemblies of LHC-II. (*a*) Cryogenic electron micrograph of a peripheral edge of the octahedral crystal of LHC-II. Small crystals of LHC-II were grown in a solution containing 50 m*M* KCl, 10 m*M* HEPES pH 7.0 and 0.6%(*w*/*v*) nonyl glucoside and rapidly cooled with liquid propane. (*b*) Cryogenic electron micrograph of a pre-crystallizing solution of LHC-II containing 20 m*M* KCl, 10 m*M* HEPES pH 7.0 and 0.6%(*w*/*v*) nonyl glucoside. The bar represents 100 nm.

Table 1
Data-collection statistics.

Values in parentheses are for the highest resolution shell.

X-ray source	BL41XU, SPring-8
Wavelength (Å)	1.0
Temperature (K)	100
Space group	*F*23
Unit-cell parameter (Å)	a = 360.6
Unique reflections	2533
Resolution range (Å)	208.2–9.5 (10.1–9.5)
Redundancy	8.0 (8.3)
Completeness (%)	99.9 (99.9)
Average $I/\sigma(I)$	3.0 (1.5)
R_{sym}†	0.085 (0.499)
Twin fraction	0.45

† $R_{sym} = \sum |I_{hkl} - \langle I_{hkl}\rangle| / \sum \langle I\rangle$, where I_{hkl} is a single value of the measured intensity of the hkl reflection and $\langle I_{hkl}\rangle$ is the mean of all measured values of the intensity of the hkl reflection.

3. Results

3.1. Spherical shell assemblies of LHC-II in the octahedral crystal

Fig. 1(*a*) shows an example of cryogenic transmission electron micrographs of a peripheral edge of a small octahedral crystal of LHC-II. This image clearly indicates that the octahedral crystal is composed of spherical shell assemblies with a diameter of 250 Å. The thickness of each spherical shell assembly is ∼50 Å, *i.e.* nearly the same as the thickness of a two-dimensional crystal of LHC-II (Kühlbrandt *et al.*, 1994). Thus, it is concluded that the spherical shell assembly found in the crystal is made up of a single layer of membrane.

The mechanism of formation of the spherical shell assembly of LHC-II was investigated by taking electron micrographs of a pre-crystallizing solution of LHC-II. Below 10 m*M* KCl no spherical shell assembly was visible in the protein/detergent/buffer solution, yet no protein was found to penetrate through a membrane filter with a molecular-sieve size of 100 kDa. This suggests that LHC-II forms trimers or larger oligomers even in the absence of KCl (data not shown). Above 20 m*M* KCl the spherical shell assembly becomes visible, as shown in Fig. 1(*b*). When the concentration of KCl exceeds 30 m*M*, octahedral crystals of LHC-II grow. The influence of KCl on protein assembly and crystal growth is explained well by the shielding effect of electrostatic repulsions between the proteins or the vesicles.

3.2. X-ray crystallographic analysis of the octahedral crystal

The octahedral crystal produced according to the protocol of Kühlbrandt (1987) diffracted to 15 Å resolution. This crystal was shown to belong to space group $P2_13$ or $P4_232$, with unit-cell parameters $a = b = c = 387$ Å (at room temperature). On the other hand, the octahedral crystal produced by our protocol belonged to space group $F23$ or $F432$, with unit-cell parameters $a = b = c = 360.6$ Å. This crystal diffracted X-rays to 8 Å resolution. It should be pointed out that there is no apparent difference in crystal shape between the $P2_13$ (or $P4_232$) crystal and the $F23$ (or $F432$) crystal. The structural analysis described below was performed using diffraction data from the $F23$ (or $F432$) crystal cooled to 100 K. The diffraction data statistics are summarized in Table 1.

To elucidate whether the vesicle has non-crystallographic symmetry axes, we calculated the self-rotation function from the diffraction data. When the calculation was performed with an integration radius of 90 Å (about 1/3 of the vesicle diameter), the rotational correlation in the Patterson space showed a set of peaks for twofold, threefold and fivefold axes. The stereographic plot derived from the rotational correlation function sectioned at $\kappa = 72^\circ$ is shown in Fig. 2. The relative positions of the correlation peaks are exactly consistent with the icosahedral symmetry.

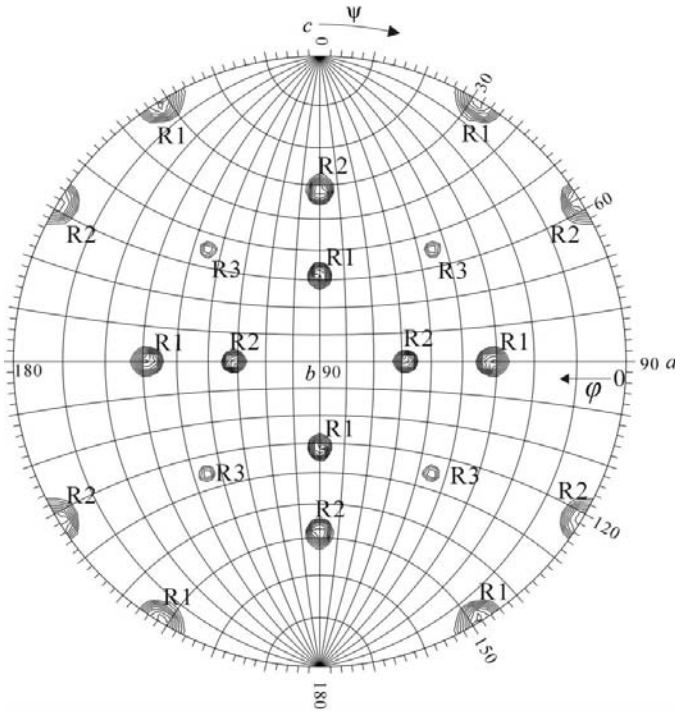

Figure 2
Stereographic projection map of the self-rotation function. The result of search for fivefold symmetry axes is shown. κ was fixed at 72° and φ and ψ were varied from 0 to 180° with a 3° interval. In this calculation, 1400 reflections between 14 and 9.5 Å resolution with $I/\sigma(I) > 3.0$ were used. The radius of integration was 90 Å. The contours are drawn at intervals of 10, starting from 530. The correlation peaks marked R1 and R2 come from the two icosahedra related by the twinning operation (*i.e.* 90° rotation of a crystal domain around a crystallographic twofold axis). The minor peaks marked R3 arise from interference between reflections from these two icosahedra; note that they can be superimposed when one icosahedron is rotated around a crystallographic threefold axis by an angle of 75.52°. The observed peaks in the self-rotation function are reproduced well when the final structural model (Fig. 5) is placed in a merohedral twin.

From closer investigation of the rotational correlation function, it was found that the crystal contains two superimposed icosahedral assemblies rotated 90° about the principal axes with respect to each other. Such orientations may be explained by supposing space group $F432$, *i.e.* eight icosahedral particles per unit cell. In this case, however, it would be calculated from the unit-cell parameter that the spherical shell has a diameter less than 150 Å. This calculated value is not compatible with the results of electron microscopy, which indicate that the centre-to-centre distance between neighbouring spherical shell assemblies is ∼250 Å. A better correlation between diffraction data and electron micrographs is found by supposing that the crystal belongs to space group $F23$ (four icosahedral particles per unit cell) and that it is merohedrally twinned. In this space group, the centre-to-centre distance between adjacent spherical shells is calculated to be 254 Å.

The intensity statistics indeed show that the crystal used is merohedrally twinned. Fig. 3 shows the cumulative distribution of the fractional difference between a pair of twin-related intensities [$I(hkl)$ and $I(hlk)$]. From the initial slope of the experimental curve in Fig. 3, the twinning fraction was estimated to be 0.45. This value means that the crystal is a nearly perfect twin. For practical reasons, the mean intensity of the hkl and hlk reflections {*i.e.* $I_{\rm twin}(hkl) = [I(hkl) + I(hlk)]/2$} was used in the following structural analysis.

3.3. Icosahedral model of LHC-II

An icosahedral model of LHC-II was constructed using the polyalanine model of LHC-II previously derived from the electron crystallographic analysis of a two-dimensional crystal of LHC-II by Kühlbrandt *et al.* (1994). According to their

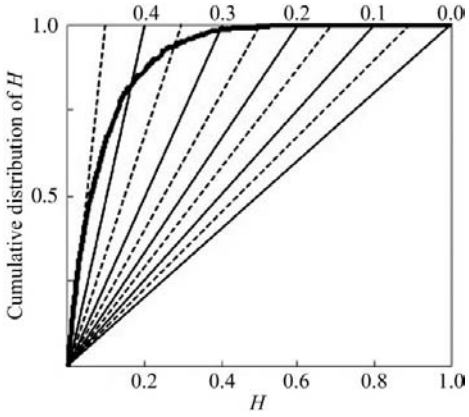

Figure 3
Estimation of the twinning fraction. The parameter H is the fractional difference between the intensities of twin-related reflections, *i.e.* $H = |I(hkl) - I(hlk)|/[I(hkl) + I(hlk)]$. The cumulative distribution of H, $S(H)$, is calculated over acentric reflections. The thick solid line is derived using data in the resolution range 20–9.5 Å from the octahedral crystal of LHC-II. From its initial slope, the twinining fraction is estimated to be 0.45. The straight thin lines are the theoretical curves expected for different values of the twinining fraction.

structural model, each monomer is composed of three transmembrane helices (*A*, *B* and *C*), a short helix (*D*) located near the lumenal surface of the membrane and 12 chlorophyll molecules. In the present model building, we assumed that the trimeric structure observed in the two-dimensional crystal is retained in the icosahedral assembly, as the preparation method employed in the present study primarily yielded trimers of LHC-II. This is also supported by the previous observations that the octahedral crystal only grows in the presence of native lipids [*i.e.* phosphatidylglycerol (PG) and digalactosyl diacylglycerol (DGDG)] (Nussberger *et al.*, 1993) and that PG is crucial for the formation of the trimeric structure of LHC-II (Krupa *et al.*, 1992).

From the ratio between the total area of the inner surface of the vesicle (100 000 Å^2) and the area occupied by each trimer (4 200 Å^2), it is reasonable to suppose that 20 trimers are arranged in an icosahedral lattice. In this case, the centre of each trimer should lie on a threefold axis. That is, the icosahedral structure can be defined by two parameters: the diameter of the icosahedron and the rotation angle of each trimer around the threefold-symmetry axis passing through the centre of the trimer. To find out the most likely structural model, we first constructed various trial models using different parameter values and then investigated the degree of fitting between the observed and the calculated intensities of diffraction. Fig. 4 shows a contour map of the crystallographic *R* factors ($R_{\rm cryst}$) evaluated for 800 trial models. When diffraction data between 18 and 9.5 Å were included in this calculation, the $R_{\rm cryst}$ value took a minimum value (0.392) when the vesicle has a radius of 134 Å at the outermost atom and the trimer was oriented in such a manner that the crevice between the neighbouring monomers is positioned on a line connecting the centres of neighbouring trimers.

The above calculation was performed on the assumption that the crystal is made up of right-side-out vesicles, *i.e.* the stromal surface (N-terminus) of the protein faces outward. When the same calculation was performed assuming inside-out vesicles, the $R_{\rm cryst}$ value did not decrease below 0.43. Thus, we conclude that the *F*23 crystal is composed of right-side-out vesicles of LHC-II. This conclusion is supported by the observation that the N-terminal region of LHC-II was cleaved upon tryptic treatment of the vesicular assemblies, which were prepared by dissolving the octahedral crystal in a solution containing 20 m*M* KCl and 10 m*M* HEPES pH 7.0 (data not shown). Our result is in line with the asymmetric charge distribution predicted by the structure model of LHC-II, *i.e.* more than 14 negatively charged residues per monomer are placed on the stromal surface.

The position and orientation of the individual monomer was further refined using rigid-body refinement. These parameters were little affected by this refinement, while the crystallographic *R* and the free *R* values decreased to 0.343 and 0.364, respectively. This result suggests that the trimeric structure of LHC-II observed in the two-dimensional crystal is retained in the icosahedral assembly.

Fig. 5(*a*) shows a view of the icosahedral model that was constructed using the parameters found in the above analysis. In this model, the closest distance (8 Å) between neighbouring trimers is seen near the inner surface (*i.e.* the lumenal surface), where the C-terminal end of helix *D* of one monomer faces toward the N-terminal end of helix *C* of another monomer (Fig. 5*b*). Since the polypeptide termini and the loops connecting the helices are truncated in the polyalanine model used in the present study, it is very likely that direct protein–protein interactions are involved in the assembly of the trimers into the icosahedral lattice. At the outer surface of the icosahedron, there is a large gap (15 Å maximum) between neighbouring trimers. This space is probably filled by lipids and/or detergents. The outermost atom of the icosahedron is 134 Å from the vesicle centre and is found at the N-terminal end of helix *A*. The closest distance from this atom to atoms in the adjacent icosahedron is 12 Å. Interactions between neighbouring icosahedra are probably mediated by amino-acid residues at the N-terminal end of helix *A* or on the loop connecting helices *A* and *C*.

The shaded arc in Fig. 5(*b*) represents a hydrophobic layer of lipid and/or detergent molecules filling the space between the proteins. This layer is hypothesized to explain the periodic variation in the diffraction intensity at low reflection angles (data not shown), which suggests the existence of a low

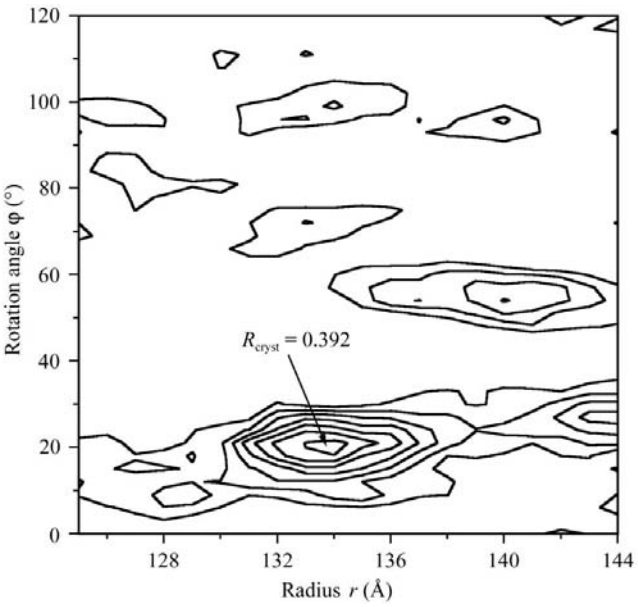

Figure 4
Contour map of the crystallographic *R* values evaluated for 800 trial icosahedral models. Each trial model was built by arranging 20 trimers in a $T = 1$ icosahedral lattice with radius r and then rotating the trimers around the threefold axes passing through their centre by an angle φ. Using the program *CNS* 1.0 (Brünger *et al.*, 1998), the structure amplitude $F_{\rm c}$ was calculated for reflections in the resolution range 18–9.5 Å and, after searching for optimal values of the scaling factor (k) and the overall temperature factor (B), the $R_{\rm cryst}$ value, defined as $\sum[k|F_{\rm c}|\exp(-B|\mathbf{s}|^2/4) - |F_{\rm o}|]/\sum|F_{\rm c}|$, was evaluated. Here, $F_{\rm o}$ is the observed structure-factor amplitude. This calculation was repeated for various values of r and φ. The results shown were obtained when the r value was increased from 125 to 144 Å using a step of 1 Å and the φ value was changed between 0 and 120° with a step of 3°. The contour lines are drawn with an interval of 0.01 in regions where $R_{\rm cryst} \leq 0.46$. The lowest $R_{\rm cryst}$ value was found at r = 134 Å and φ = 19°.

electron-density region with a thickness of 20 Å (Hino, 2003). (Details will be described elsewhere.)

4. Discussion

The present results demonstrate that the octahedral crystal of LHC-II is made up of hollow spherical assemblies, each containing 20 protein trimers arranged in a $T = 1$ icosahedral lattice. This is the second example of a membrane protein that forms polyhedral assemblies under crystallization conditions. The first example was observed in the $P6_322$ crystal of bacteriorhodopsin (Kouyama *et al.*, 1994). Our recent study of the octahedral $F23$ crystal of bacteriorhodopsin vesicles suggests that 420 trimers are arranged in a $T = 7$ icosahedral lattice with a diameter of 460 Å (A. Horigome, T. Nishikawa & T. Kouyama, unpublished data). These observations are not surprising as the arrangement of trimeric lipid–protein complexes on an icosahedral lattice is geometrically and energetically allowed.

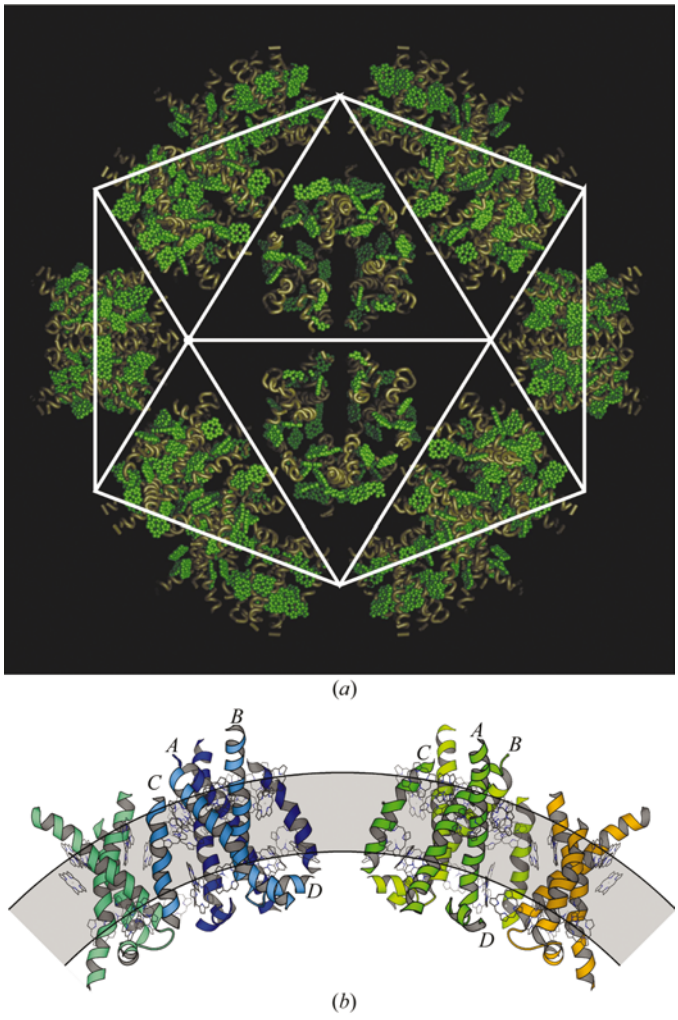

Figure 5
Structure of the icosahedral assembly of LHC-II. (*a*) View of the whole assembly along a twofold symmetry axis, overlaid on a $T = 1$ icosahedral lattice (white line). Polypeptides are drawn in a ribbon representation (gold) and chlorophylls are drawn in CPK representation (green). (*b*) Enlarged view showing the relative positions of neighbouring trimers. Each subunit of the protein is composed of three transmembrane helices (*A*, *B* and *C*) and a short helix (*D*) located near the lumenal surface of the membrane and 12 chlorophyll molecules (shown as a wire model). The shaded arc represents a hypothetical hydrophobic region of the lipid–detergent bilayer. (*a*) was drawn with *VMD* (Humphrey *et al.*, 1996) and *POV-Ray* (http://www.povray.org) and (*b*) with *MOLSCRIPT* (Kraulis, 1991) and *RASTER3D* (Merritt & Murphy, 1994).

Nussburger *et al.* (1993) reported that the presence of two types of native lipid [*i.e.* phosphatidylglycerol (PG) and digalactosyl diacylglycerol (DGDG)] is essential for the growth of the octahedral crystal. On the other hand, it was previously observed that only one of them (PG) is required for formation of the trimeric structure of LHC-II (Krupa *et al.*, 1992). One possible explanation of these observations is that DGDG is distributed around the trimeric structure of LHC-II and mediates interactions between adjacent LHC-II trimers in the icosahedral structure. This possibility is supported by the observation that the LHC-II icosahedral shell contains a thin layer that has a lower electron density than that of the bulk solvent (Hino, 2003). It is very likely that the space between the LHC-II trimers in the icosahedral structure is filled completely with lipids and/or detergents, *i.e.* the LHC-II icosahedron is a closed proteoliposome.

The LHC-II icosahedral vesicle is much smaller than the bacteriorhodopsin vesicle or the smallest vesicles of pure lipids. A special driving force must exist that makes the LHC-II vesicle very small. This force is probably not related to the shape of the trimeric structure of LHC-II, which is approximated by a rod rather than by a cone. A more likely cause is an asymmetric charge distribution in the protein. According to the structural model of LHC-II derived by electron crystallography (Kühlbrandt *et al.*, 1994), negatively charged residues are abundant on the protein surface at the stromal side. Our model of the icosahedral vesicle indicates that this surface faces outward (Fig. 5*b*). Since the LHC-II vesicles are formed at a low salt concentration (20 m*M* KCl), electrostatic fields originating from negatively charged residues on the stromal surface are not sufficiently shielded out. Given the trimer–trimer contact at the lumenal side, the electrostatic repulsion between the stromal surfaces can be reduced by increasing the membrane curvature. In order for the LHC-II vesicles to be stacked into the octahedral crystals, electrostatic repulsion between the vesicles must be reduced by the addition of salt. This effect was observed experimentally (Fig. 1).

The icosahedral vesicle of LHC-II is produced by a simple procedure. It is interesting to ask why the icosahedral vesicle of LHC-II has not been observed under physiological conditions. It could be argued that the formation of such a vesicle is functionally makes no sense, as efficient energy transfer from LHC-II to the reaction centre of photosystem II is only achieved when these membrane proteins exist in the same thylakoid membrane; however, this argument does not exclude the possibility that the vesicle formation of LHC-II is involved in a developmental process of the thylakoid membranes in plant chloroplasts. Judging from the ease with which LHC-II forms vesicles, we suppose that any membrane proteins with asymmetric charge distributions will form vesi-

cular assemblies if they are segregated, for example, from lipid-rich regions in a membrane (Simons & Ikonen, 1997). It would be valuable to investigate whether other membrane proteins are able to self-assemble into regular polyhedral structures under some solvent conditions, as such a protein assembly could be used to purify a specific membrane protein without complete solubilization of the biological membrane.

The octahedral crystal used in the present structural analysis is morphologically similar to, but crystallographically different from, the crystal prepared according to the protocol of Kühlbrandt (1987). The latter belongs to space group $P2_13$ and its unit-cell parameter (387 Å) is slightly larger than that of the $F23$ crystal we obtained. It should be mentioned that below 30 Å resolution the diffraction pattern from the $P2_13$ crystal was characterized by very weak reflections at the Miller indices $h + k \neq 2n$, $k + l \neq 2n$ or $l + h \neq 2n$ (data not shown). This implies that the $P2_13$ crystal has pseudo-face-centred symmetry at low resolution. We suppose that the $P2_13$ crystal is made up of spherical shell assemblies as found in the $F23$ crystal. In this case, alteration in the space group can be explained by a small reorientation of the spherical shell assemblies in the unit cell, *i.e.* the $F23$ crystal is converted to the $P2_13$ crystal when the four vesicles in the unit cell are rotated systematically around the crystallographic threefold axes. This interpretation is supported by our observation that the space group often changed when diffraction data from a single crystal were collected at room temperature.

We wish to express our gratitude to Dr Kühlbrandt for providing us with a coordinate file for the C^{α} and chlorophyll porphyrin rings of LHC-II, Drs M. Kawamoto and K. Miura for helping with data collection at beamlines BL41XU and BL40B2 of SPring-8 (proposal Nos. 1999B0258-NL-np, 2000B0449-NL-np, 2001A0491-CL-np, 2002A0420-NL-np and 2002B0516-NL1-np) and Mr T. Goto for technical advice on electron microscopy. This work was supported in part by National Project on Protein Structural and Functional Analyses and by Grants-in-Aid from the Ministry of Education, Science and Culture of Japan.

References

Arnon, D. I. (1949). *Plant Physiol.* **24**, 1–15.
Brandstetter, H., Jeong-Sun, K., Groll, M. & Huber, R. (2001). *Nature (London)*, **414**, 466–470.
Brünger, A. T., Adams, P. D., Clore, G. M., DeLano, W. L., Gros, P., Grosse-Kunstleve, R. W., Jiang, J.-S., Kuszewski, J., Nilges, M., Pannu, N. S., Read, R. J., Rice, L. M., Simonson, T. & Warren, G. L. (1998). *Acta Cryst.* D**54**, 905–921.
Burke, J. J., Ditto, C. L. & Arntzen, C. J. (1978). *Arch. Biochem. Biophys.* **187**, 252–263.
Casper, D. & Klug, A. (1963). *Cold Spring Harbor Symp. Quant. Biol.* **27**, 1–4.
Collaborative Computational Project, Number 4 (1994). *Acta Cryst.* D**50**, 760–763.
Crowther, R. A., Amos, L. A., Finch, J. T., DeRosier, D. J. & Klug, A. (1970). *Nature (London)*, **226**, 421–425.
Domingo, G. J., Orru', S. & Perham, R. N. (2001). *J. Mol. Biol.* **305**, 259–267.
Forsell, K., Xing, L., Kozlovska, T., Cheng, R. H. & Garoff, H. (2000). *EMBO J.* **19**, 5081–5091.
Heinz, F. X. & Allison, S. L. (2001). *Curr. Opin. Microbiol.* **4**, 450–455.
Hino, T. (2003). PhD thesis. Graduate School of Science, Nagoya University, Japan.
Humphrey, W., Dalke, A. & Schulten, K. (1996). *J. Mol. Graph.* **14**, 33–38.
Izard, T., Aevarsson, A., Allen, M. D., Westphal, M. D., Perham, R. N., de Kok, A. & Hol, W. G. (1999). *Proc. Natl Acad. Sci. USA*, **94**, 1240–1245.
Kouyama, T., Yamamoto, M., Kamiya, N., Iwasaki, H., Ueki, T. & Sakurai, I. (1994). *J. Mol. Biol.* **236**, 990–994.
Kraulis, P. J. (1991). *J. Appl. Cryst.* **24**, 946–950.
Krupa, Z., Williams, J. P., Mobashoher, U. K. & Huner, N. P. A. (1992). *Plant Physiol.* **100**, 931–938.
Kühlbrandt, W. (1987). *J. Mol. Biol.* **194**, 757–762.
Kühlbrandt, W. (1994). *Curr. Opin. Struct. Biol.* **4**, 519–528.
Kühlbrandt, W., Wang, D. N. & Fujiyoshi, Y. (1994). *Nature (London)*, **367**, 614–621.
McRee, D. E. (1993). *Practical Protein Crystallography*. San Diego, USA: Academic Press.
Matsui, Y., Sakai, K., Murakami, M., Shiro, Y., Adachi, S., Okumura, H. & Kouyama, T. (2002). *J. Mol. Biol.* **324**, 469–481.
Merritt, E. A. & Murphy, M. E. P. (1994). *Acta Cryst.* D**50**, 869–873.
Nussberger, S., Dörr, K., Wang, D. N. & Kühlbrandt, W. (1993). *J. Mol. Biol.* **234**, 347–356.
Pearse, B. M., Smith, C. J. & Owen, D. J. (2000). *Curr. Opin. Struct. Biol.* **10**, 220–228.
Persson, K., Schneider, G., Jordan, D. B., Viitanen, P. V. & Sandalova, T. (1999). *Protein Sci.* **8**, 2355–2365.
Sato, H., Takeda, K., Tani, K., Hino, T., Okada, T., Nakasako, M., Kamiya, N. & Kouyama, T. (1999). *Acta Cryst.* D**55**, 1251–1256.
Simons, K. & Ikonen, F. (1997). *Nature (London)*, **387**, 569–572.
Smith, C. J., Grigorieff, N. & Pearse, B. M. (1998). *EMBO J.* **17**, 4943–4953.
Steller, I., Bolotovsky, B. & Rossmann, M. G. (1997). *J. Appl. Cryst.* **30**, 1036–1040.
Takeda, K., Sato, H., Hino, T., Kono, M., Fukuda, K., Sakurai, I., Okada, T. & Kouyama, T. (1998). *J. Mol. Biol.* **283**, 463–474.
Tong, L. & Rossmann, M. G. (1990). *Acta Cryst* A**46**, 783–792.
Walz, J., Koster, A. J., Tamura, T. & Baumeister, W. (1999). *J. Struct. Biol.* **128**, 65–68.
Wilson, A. J. C. (1949). *Acta Cryst.* **2**, 318–321.
Yeates, T. O. (1997). *Methods Enzymol.* **276**, 344–358.
Zhang, X., Meining, W., Fischer, M., Bacher, A. & Ladenstein, R. (2001). *J. Mol. Biol.* **306**, 1099–1114.